Mechanism for stamp collapse in soft lithography

W. Zhou and Y. Huang[a)]
Department of Mechanical and Industrial Engineering, University of Illinois at Urbana-Champaign, Urbana, Illinois 61801

E. Menard
Department of Materials Science and Engineering, University of Illinois at Urbana-Champaign, Urbana, Illinois 61801

N. R. Aluru
Department of Mechanical and Industrial Engineering, University of Illinois at Urbana-Champaign, Urbana, Illinois 61801

J. A. Rogers[a)]
Department of Materials Science and Engineering, University of Illinois at Urbana-Champaign, Urbana, Illinois 61801

A. G. Alleyne
Department of Mechanical and Industrial Engineering, University of Illinois at Urbana-Champaign, Urbana, Illinois 61801

(Received 5 October 2005; accepted 16 November 2005; published online 14 December 2005)

Mechanical collapse of recessed features of relief on elastomeric elements for soft lithography represents an important phenomena for this lithographic technology. By comparing computed and measured shapes of partially collapsed structures, we show that the dominant mechanism for collapse is surface adhesion between the elastomer and substrate, for typical materials and processing conditions. In particular, the shapes obtained using models that account for surface adhesion agree well with the experimentally measured shapes. Electrostatic forces may contribute to this process, but they do not dominate. The weight of the elastomer has essentially no effect.
© *2005 American Institute of Physics*. [DOI: 10.1063/1.2149513]

Soft lithography refers to a class of patterning techniques that has promising applications in areas, such as plastic electronics, fiber optics, and microfluidics. In printing based soft lithographic methods, an ink is transferred to a substrate by bringing an elastomeric element, known as the stamp, with suitable patterns of surface relief into contact with the substrate surface. In other approaches, this type of element provides a conformable photomask for patterning photoresist or a structure of patterned electrodes for electronic devices. References 1 and 2 provide reviews of recent developments in soft lithography. In all cases, intimate physical contact between the elastomer and substrate is critically important. The elastomer is most commonly some form of poly(dimethylsiloxane) (PDMS), which is easily deformable with the shear modulus $\mu \leqslant 1$ MPa.[3] Partly because of this low stiffness, the stamp is able to form conformal contacts to substrates, with modest or no applied pressure. Although necessary in the raised regions of relief, this contact usually represents an unwanted parasitic effect when it occurs in the recessed areas. Such behavior, which we refer to as "roof collapse," can be observed with or without external loading.[3] The phenomena are schematically illustrated in Fig. 1. For the studies described here, the stamp surface consists of flat punches whose width $2w$ and spacing $2a$ (Fig. 1) are on the order of tens to hundreds of microns. The height h of the flat punches is much smaller, on the order of microns. For such small punch height h, roof collapse may occur without any external load.[4,5] We used an optical method based on Fizeau's interference fringes to measure the gap profile of the unsagged part between PDMS and the substrate.[6] When the gap profile of a PDMS stamp laminated against a flat silicon wafer is observed under a high resolution microscope, local interference fringes are observed. Figure 2(b) (top) shows measured light intensity for a PDMS stamp, with small punch spacing ($2a \ll 2w$), in contact with a silicon wafer. Figure 2(b) (bottom) also shows the reconstructed gap profile where y represents the gap, x is the coordinate with origin at the collapsed end, and punch height $h=3.21$ μm($\ll 2a$). Several possible mechanisms may be responsible for this behavior, including (1) surface adhesion between PDMS and the substrate; (2) electrostatic force; and (3) weight of PDMS. In this letter, we study the gap profiles from theoretical models

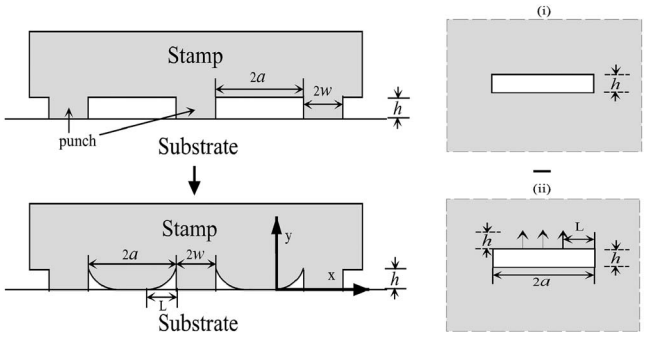

FIG. 1. A schematic diagram of roof collapse for a stamp on substrate in soft lithography, and a schematic diagram to illustrate roof collapse as the difference between (i) the ground state and (ii) a state with constant opening displacement h around the center.

[a)]Authors to whom correspondence should be addressed; electronic mail: huang9@uiuc.edu, jrogers@uiuc.edu

 © 2005 American Institute of Physics
Downloaded 13 Jan 2006 to 130.126.121.152. Redistribution subject to AIP license or copyright, see http://apl.aip.org/apl/copyright.jsp

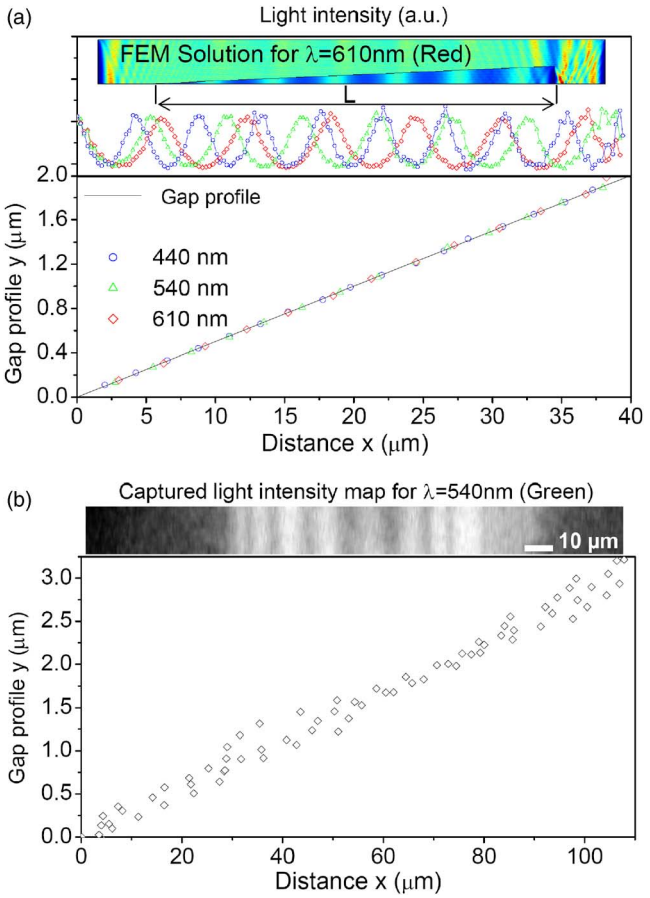

FIG. 2. Fizeau's interference fringes located in the sagging area of a PDMS stamp laminated against a flat substrate. (a) Finite element modeling and gap profile reconstruction in the case of a linear sagging profile. (b) The top part shows the light intensity map of a sagging stamp for an incoming white light filtered using a narrow-band optical filter (λ=540±5 nm). The bottom part shows the reconstructed profile using three narrow-band filters with 440, 540, and 610 nm center wavelengths.

for these three mechanisms of roof collapse and compare them with the experimentally measured profile in Fig. 2 in order to determine the dominant mechanism for roof collapse.

For very small punch height $h \ll 2a$, the thin gap between PDMS and the substrate can be considered as a crack[7] as illustrated in Fig. 1. The collapsed state with the gap length L can be considered as the *difference* between (i) the ground state without collapse and (ii) a constant *opening* displacement h over the collapsed part. The state (ii) can be approximated by a *crack* with constant opening displacement h around the center, for which the analytic solution of stress and deformation fields exists.[8] Such an approach gives the gap length via energy minimization as $L=Eh^2/(3\pi\gamma)$, which agrees very well with the gap length measured from experiments,[7] where E is the Young's modulus of PDMS, and γ is the adhesion energy between PDMS and the Si substrate.

We follow the same approach[7] but focus on the gap profile in this letter. Without accounting for surface adhesion or electrostatic force, the unsagged part of the surface remains traction free. The gap profile can then be obtained analytically as[7,8]

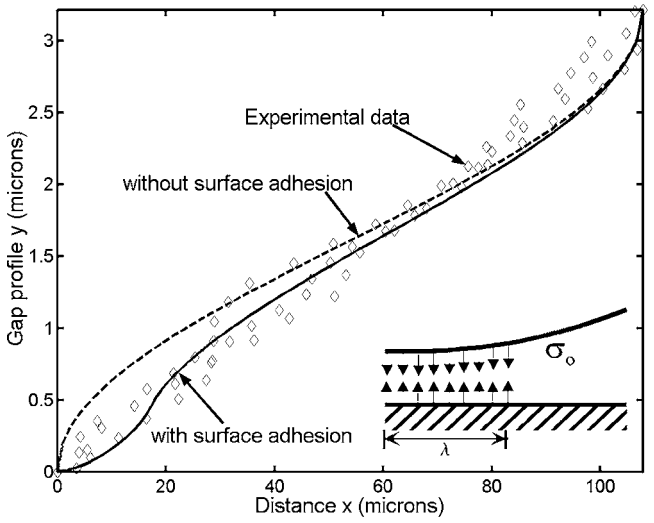

FIG. 3. The gap profiles with and without surface adhesion, and the experimentally measured profile. The punch height $h=3.21$ μm, gap length $L=108$ μm, and adhesion strength $\sigma_0=36$ KPa.

$$y_0 = h - h\frac{2}{\pi}\sin^{-1}\sqrt{\frac{L-x}{L}}. \tag{1}$$

Such a profile gives a singular stress field around $x=0$ (the tip separating the sagged and unsagged parts), and the corresponding stress intensity factor is $K=\sqrt{2}Eh/(3\sqrt{\pi L})$.[8] As shown in Fig. 3, the gap profile in Eq. (1) does not agree well with that measured from experiments, particularly near $x=0$. This discrepancy results from the traction-free assumption over the unsagged part, which neglects the surface adhesion or electrostatic force. For example, the surface adhesion does not vanish near $x=0$ where the PDMS and the substrate surfaces are rather close.

We first investigate the effect of surface adhesion on the gap profile. The adhesion is near $x=0$ (where the sagged and unsagged parts separate), and it can be represented by a constant adhesion strength σ_0 over a region of length $\lambda(0<x<\lambda)$, as shown schematically in the inset of Fig. 3. Similar to the Dugdale model in fracture mechanics,[9] the length of ad-

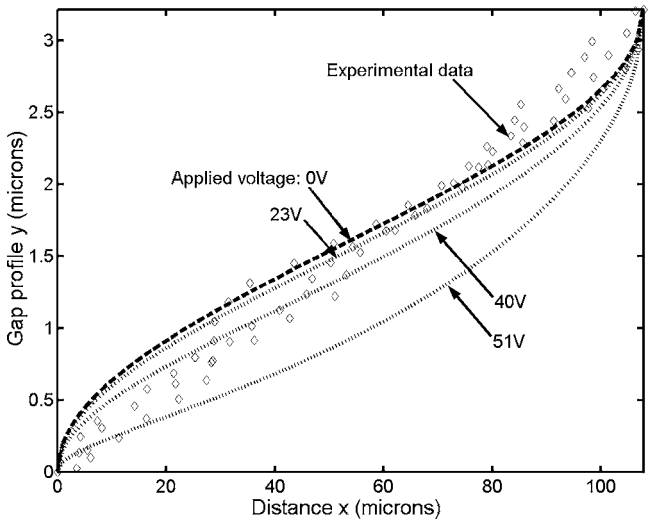

FIG. 4. The gap profiles for different applied voltage, and the experimentally measured profile. The punch height $h=3.21$ μm and gap length $L=108$ μm.

Downloaded 13 Jan 2006 to 130.126.121.152. Redistribution subject to AIP license or copyright, see http://apl.aip.org/apl/copyright.jsp

hesion zone λ is determined by eliminating the stress singularity around the crack tip $x=0$ as[8]

$$K-\sigma_0\sqrt{\frac{L}{2\pi}}\left[\cos^{-1}\left(1-\frac{2\lambda}{L}\right)+2\sqrt{\frac{\lambda}{L}-\frac{\lambda^2}{L^2}}\right]=0, \qquad (2)$$

where K is the aforementioned stress intensity factor for the gap profile in Eq. (1). For small punch height $h \ll L$, λ is given by $\lambda=\pi K^2/(8\sigma_0^2)$, or in terms of the punch height as $\lambda=E^2h^2/(36\sigma_0^2L)$.

The gap profile due to surface adhesion then becomes

$$y=y_0-\frac{2h}{\pi L}\frac{\cos^{-1}\left(1-\frac{2\lambda}{L}\right)\sqrt{Lx-x^2}+(\lambda-x)\cosh^{-1}\left|\frac{L(\lambda+x)-2\lambda x}{L(\lambda-x)}\right|}{\cos^{-1}\left(1-\frac{2\lambda}{L}\right)+2\sqrt{\frac{\lambda}{L}-\frac{\lambda^2}{L^2}}}, \qquad (3)$$

where y_0 is the profile in Eq. (1), and the last term in Eq. (3) represents the closure due to surface adhesion over length λ.[8] Figure 3 compares the gap profile in Eq. (3) with the experimentally measured profile. The punch height and gap length are measured from experiments as $h=3.21$ μm and $L=108$ μm. The adhesion strength is taken as $\sigma_0=36$ kPa, which is slightly above 1% of the Young's modulus of PDMS (2.8 MPa) (Refs. 4 and 5) and has the correct order of magnitude. This gives to the adhesion zone length $\lambda=17.2$ μm. The gap profile in Eq. (3) accounting for surface adhesion agrees well with the experimentally measured profile.

We now investigate the effect of electrostatic force on the gap profile. The stamp and substrate surfaces may have opposite electric charges to bring the surfaces closer, $y=y_0-y_{\text{electric}}$, where y_{electric} is related to the stress traction σ_{electric} on stamp and substrate surfaces (due to electric charges) via the Green's function,[8] and σ_{electric} can be obtained from the parallel plate capacitor problem in electrostatics as[10,11]

$$\sigma_{\text{electric}}=\frac{\varepsilon_0 V^2}{2\bar{y}^2}. \qquad (4)$$

Here $\varepsilon_0=8.8542\times10^{-12}$ C^2 N^{-1} m^{-2} is the permittivity of free space, V is the applied voltage, and $\bar{y}=\int_0^L y\,dx/L$ is average gap between the stamp and substrate. Such an approach gives the gap profile due to electrostatic force as

$$y=y_0-\frac{3\varepsilon_0 V^2}{2E\bar{y}^2}\sqrt{Lx-x^2}, \qquad (5)$$

where the average gap $\bar{y}$ is determined by averaging both sides of Eq. (5) over length L, which gives $\bar{y}=h/2-3\pi L\varepsilon_0 V^2/(16E\bar{y}^2)$.

The gap profile in Eq. (5) is shown in Fig. 4 for applied voltage $V=0$, 23, 40, and 51 V, where $V=0$ corresponds to the profile in Eq. (1). The experimentally measured profile is also shown for comparison. The punch height h, gap length L, and Young's modulus of PDMS E are same as those in Fig. 3. Even for such a wide range of applied voltage, the gap profile in Eq. (5) accounting for electrostatic forces does not agree with the experimentally measured profile.

The weight of PDMS has essentially no effect on roof collapse. For a very thick PDMS layer of 10 mm, the maximum displacement at the gap is only 50 nm, which is too small as compared to the punch height h (a few microns). Therefore, the weight of a PDMS cannot be responsible for roof collapse.

In summary, the surface adhesion is responsible for roof collapse of PDMS stamp. Electrostatic force may contribute, but it is not the dominant mechanism for roof collapse. The weight of PDMS has essentially no effect.

The authors acknowledge the financial support from the NSF through Nano-CEMMS (Grant No. DMI 03-28162) at the University of Illinois. Y.H. also acknowledges the support from NSFC.

[1] J. A. Rogers and R. G. Nuzzo, Mater. Today **8**, 50 (2005).
[2] J. W. P. Hsu, Mater. Today **8**, 42 (2005).
[3] C. Y. Hui, A. Jagota, Y. Y. Lin, and E. J. Kramer, Langmuir **18**, 1394 (2002).
[4] K. G. Sharp, G. S. Blackman, N. J. Glassmaker, A. Jagota, and C. Y. Hui, Langmuir **20**, 6430 (2004).
[5] K. J. Hsia, Y. Y. Huang, E. Menard, J.-U. Park, W. Zhou, J. A. Rogers, and J. M. Fulton, Appl. Phys. Lett. **86**, 154106 (2005).
[6] M. V. Klein and T. E. Furtak, *Optics* (Wiley, New York, 1986).
[7] Y. Y. Huang, W. Zhou, K. J. Hsia, E. Menard, J.-U. Park, J. A. Rogers, and A. G. Alleyne, Langmuir **21**, 8058 (2005).
[8] H. Tada, P. C. Paris, and G. R. Irwin, *The Stress Analysis of Cracks Handbook*, 3rd ed. (ASME, New York, 2000).
[9] T. L. Anderson, *Fracture Mechanics, Fundamentals, and Applications* (CRC Press, Cleveland, 1995).
[10] N. R. Aluru, Comput. Mech. **23**, 324 (1999).
[11] M. Dequesnes, S. Rotkin, and N. R. Aluru, Nanotechnology **13**, 120 (2002).

Downloaded 13 Jan 2006 to 130.126.121.152. Redistribution subject to AIP license or copyright, see http://apl.aip.org/apl/copyright.jsp